Current Research in Food Science 8 (2024) 100770

Contents lists available at ScienceDirect

Current Research in Food Science

journal homepage: www.sciencedirect.com/journal/current-research-in-food-science

Enhancement of resistant starch content in ethyl cellulose-based oleogels cakes with the incorporation of glycerol monostearate

Xiaohan Chen [a], Dongming Lan [a], Daoming Li [c], Weifei Wang [b,*], Yonghua Wang [a,**]

[a] Department of Food Science and Engineering, School of Food Science and Engineering, South China University of Technology, Guangzhou, 510640, China
[b] Sericultural & Agri-Food Research Institute, Guangdong Academy of Agricultural Sciences, Key Laboratory of Functional Foods, Ministry of Agriculture and Rural Affairs, Guangdong Key Laboratory of Agricultural Products Processing, Guangzhou, 510610, China
[c] School of Food and Biological Engineering, Shaanxi University of Science and Technology, Xi'an, 710021, China

ARTICLE INFO

Handling editor: A.G. Marangoni

Keywords:
Diacylglycerol oil
Oleogel
Lipid-amylose complexes
Starch digestibility

ABSTRACT

The objective of this work was to completely replace margarine with peanut diacylglycerol oil/ethyl cellulose-glycerol monostearate oleogel (DEC/GMS) oleogel, and evaluate its effect on starch digestibility of cakes. The in vitro digestibility analysis demonstrated that the DEC/GMS-6 cake exhibited a 26.36% increase in slowly digestible starch (SDS) and resistant starch (RS) contents, compared to cakes formulated with margarine. The increased SDS and RS contents might mainly be due to the hydrophobic nature of OSA-wheat flour, which could promote the formation of lipid-amylose complexes with GMS and peanut diacylglycerol oil. XRD pattern suggested that the presence of GMS in DEC-based oleogels facilitated the formation of lipid-amylose complexes. The DSC analysis revealed that the addition of GMS resulted in a significant increase in gelatinization enthalpy, rising from 249.7 to 551.9 J/g, which indicates an improved resistance to gelatinization. The FTIR spectra indicated that the combination of GMS could enhance the hydrogen bonding forces and short-range ordered structure in DEC-based cakes. The rheological analysis revealed that an increase in GMS concentration resulted in enhanced viscoelasticity of DEC-based cake compared to TEC-based cakes. The DEC-based cakes exhibited a more satisfactory texture profile and higher overall acceptability than those of TEC-based cakes. Overall, these findings demonstrated that the utilization of DEC-based oleogel presented a viable alternative to commercial margarine in the development of cakes with reduced starch digestibility.

1. Introduction

Currently, the use of oleogel as a margarine substitute is an active area of research in the bakery industry (Roufegarinejad et al., 2023). This is owing to the high levels of saturated and trans fatty acids found in margarine, which have been associated with various adverse health outcomes in humans (Aliasl Khiabani, Tabibiazar, Roufegarinejad, Hamishehkar and Alizadeh, 2020). However, it has been discovered that the substitution of margarine with oleogel enhanced the digestibility of starch in bakery food (Alvarez-Ramirez et al., 2020; Barragán-Martínez et al., 2022). The increased digestibility of starch is closely associated with the increase in and prevalence of human health conditions, such as obesity (Li et al., 2023), diabetes (Zhang et al., 2023), and cardiovascular disease (Xu et al., 2023). Therefore, the research on reducing starch digestibility is of significant importance for oleogel-based bakery food.

Peanut diacylglycerol oil (PDO) based oleogel plays an important role in reducing the digestibility of bakery products, that can improve insulin resistance and lower blood lipid levels due to its high oleic acid content (Lei et al., 2018; Zhi-hao, Ai-min, Rui, Hong-zhi, Hui and Qiang, 2022). Our previous research has discovered that the PDO-based oleogel, which consists of ethyl cellulose (EC) and glycerol monostearate (GMS), can potentially serve as a substitute for margarine in cake formulations (Chen et al., 2023). Glycerol monostearate (GMS) was proved to possess a tailoring capacity for the structural, rheological and tribological properties of ethylcellulose (EC)-based oleogels/oleogel emulsions (Garcia-Ortega et al., 2021; Rupp and Cramer, 2022; Zhang et al., 2022). However, limited research has been conducted on the influence of GMS in oleogels on the starch digestibility of cakes. Many studies have demonstrated that lipids, such as fatty acids (Cervantes-Ramirez et al.,

* Corresponding author.
** Corresponding author.
E-mail address: wangweifei@gdaas.cn (W. Wang).

https://doi.org/10.1016/j.crfs.2024.100770
Received 5 March 2024; Received in revised form 9 May 2024; Accepted 14 May 2024
Available online 15 May 2024

2020), GMS (Kawai et al., 2012; Wang et al., 2023) and diacylglycerols (Feng et al., 2024), can form complexes with amylose to create lipid-amylose complexes. These complexes are characterized by a more stable and compact ordered structure, which leads to reduced susceptibility to enzyme decomposition and ultimately contributes to a decrease in starch digestibility (Liu et al., 2023). Therefore, investigating the relationship between lipid-amylose complexes and starch digestibility holds significant importance in oleogel-based bakery food. However, investigating lipid-amylose complexes poses several challenges. For example, the tight arrangement and difficult depolymerization of amylose, as well as the large molecular weight and steric hindrance of diacylglycerols, moderately affect the formation of complexes (Wang et al., 2021). To address these issues, one approach is the esterification modification of wheat flour using octenyl succinic anhydride (OSA), which can enhance its hydrophobicity. The United States Food and Drug Administration (FDA) has granted approval for the maximum allowable concentration of OSA to be limited to 3% (w/w starch basis) (Zheng et al., 2024). The OSA-wheat flour helix cavity could create a favorable environment for accommodating the hydrocarbon chain of the lipid molecule through a series of non-covalent interactions, due to its hydrophobic nature (Chen et al., 2022). The esterification of OSA for starch modification, as discovered by Liu et al. (2022), has been found to significantly enhance the formation of complexes between OSA-starch and linoleic acid, resulting in enhanced resistance to digestion. Although extensive investigations have been conducted on the formation of lipid-amylose complexes within OSA-starch and fatty acids, there remains a lack of studies focusing on the interaction between GMS and OSA-wheat flour. Additionally, an unexplored examination of the influence of GMS in PDO-based oleogel on starch digestibility in cake is needed.

The objective of this study was to assess the effects of substituting margarine with PDO-based oleogel on the starch digestibility in cakes. The effect of oleogels on the digestibility of cakes was investigated by measuring the levels of rapidly digestible starch (RDS), slowly digestible starch (SDS), and resistant starch (RS). The underlying mechanism of oleogels on the digestibility of cakes was elucidated through comprehensive analysis techniques including X-ray diffraction (XRD), differential scanning calorimetry (DSC), Fourier transform infrared spectroscopy (FTIR), and rheological analysis.

2. Materials and methods

2.1. Materials

Peanut triacylglycerol oil (PTO, 4.16% DAG, 93.55% TAG, 11.55% C16:0, 3.86% C18:0, 40.33% C18:1 and 38.2% C18:2) and peanut diacylglycerol oil (PDO, 81.27% DAG, 18.73% TAG, 10.95% C16:0, 3.26% C18:0, 41.09% C18:1 and 37.55% C18:2) were provided by Guangdong Yue-shan Special Nutrition Technology Co., Ltd. (Guangdong, China), ethyl cellulose (EC) (viscosity 46 cP; 5% in toluene/ethanol 80:20 (v/v); 48% ethoxy, Tg = 120 °C), glycerol monostearate (GMS), α-amylase and pepsin were provided by Yuanye Bio-Technology Co., Ltd. (Shanghai, China). Margarine (69.83% saturated fatty acid) and wheat flour (carbohydrate 76.50%, protein: 8.00%, fat:1.6%) were obtained at a local Walmart supermarket (Guangdong, China). All other chemical reagents, which were analytically pure, were provided by Aladdin Biochemical Technology Co., Ltd. (Shanghai, China). Distilled water was used in all formulations.

2.2. Preparation of OSA-wheat flour

The OSA-wheat flour preparation was conducted according to the method of Liu et al. (2022) with some modifications. Wheat flour was dispersed in distilled water (35% w/w) under continuous stirring for approximately 10 min. Subsequently, octenyl succinic anhydride (7% of wheat flour, dry weight) was added dropwise after achieving even dispersion. The entire reaction was maintained at a pH of 8.5 and a temperature of 35 °C. To terminate the reaction, the pH of the slurry was adjusted to 6.5 by adding dilute HCl. The mixture underwent centrifugation (5000×*g*, 10 min), followed by 3 washes with distilled water and 3 washes with 95% ethanol. The resulting precipitate was dried in an oven at 45 °C for 24 h and stored in a dryer for further analysis. The designated names for the resulting precipitate was OSA-wheat flour.

2.3. Preparation of oleogel

The oleogel was prepared following the method of Adili (2020) with some modifications. Different contents of EC and GMS powders (EC-GMS: 6 wt%-0 wt%; 4 wt%-2 wt%; 2 wt%-4 wt%; 0 wt%-6 wt%) were added to peanut triacylglycerol oil or peanut diacylglycerol oil, followed by heating at a constant stirring rate of 120 °C for 2 h. Subsequently, the oleogels were refrigerated at 4 °C for 24 h before being transferred to a temperature of 20 °C for analysis (Rodriguez-Hernandez, 2021). Depending on the concentration of EC and GMS, the oleogels were designated as TEC, TEC/GMS-2, TEC/GMS-4, TEC/GMS-6, DEC, DEC/GMS-2, DEC/GMS-4 and DEC/GMS-6.

2.4. Preparation of cakes

The cake was prepared following the method described by Adili (2020) with certain modifications. The foaming protein was vigorously mixed with 300 g of egg albumen and 100 g of sugar. For cake preparation, a mixture of margarine (3 g), OSA-satrch (5 g), water (5 g) and foaming protein (20 g) was used. In the formulated cakes, margarine was substituted with TEC-based and DEC-based oleogels. Subsequently, the cake batter was baked at 180 °C for 20 min in a convection oven (Midea Kitchen Appliance Manufacturing, Foshan, China) (Adili, 2020). Based on the type of oleogels employed, the cakes were designated as Margarine cake, TEC cake, TEC/GMS-2 cake, TEC/GMS-4 cake, TEC/GMS-6 cake, DEC cake, DEC/GMS-2 cake, DEC/GMS-4 cake and DEC/GMS-6. The rest of Margarine, TEC-based and DEC-based cake batters were used for determination of rheological propertie. The cakes for each formulation were prepared thrice, with three samples per batch for subsequent measurements.

2.5. Peroxide value (PV)

The peroxide value (PV) of oils was determined according to Sivakanthan et al. (2024) with some modifications. Briefly, 2 ± 0.05 g of oleogels was weighed into a 250 mL Erlenmeyer flask, and 30 mL of chloroform:acetic acid (2:3, v/v) was added and mixed well to dissolve the sample. Then, 1 mL of saturated KI solution was added, stoppered, and left to stand for 3 min in the dark with occasional shaking. Then, 100 mL of distilled water was added and titrated with 0.01 mol/L sodium thiosulfate using the starch in dicator. A blank determination also was conducted in parallel. The results was calculated by the following equation (1):

$$\mathrm{PV(mmol/kg)} = \frac{(V - V_0) \times 1000c}{2M} \quad (1)$$

where V and V_0 was the volume of sodium thiosulfate solution consumed of the test solution and the reagent blank, c was the concentration of sodium thiosulfateand, M was the weight of the sample.

2.6. The 2-thiobarbituric acid (TBA)

The 2-thiobarbituric acid (TBA) value was determined according to the method of Zhao et al. (2023). Briefly, the samples containing 200 mg of oleogels were dissolved in n-butanol and fixed to 25 mL. An amount of 5 mL of this solution was then mixed with 5 mL of 0.2% TBA reagent and incubated in a water bath at 95 °C for 2 h. A blank determination also

was conducted in parallel. The absorbance was measured at 530 nm, and the TBA value was calculated by the following equation (2):

$$\text{TBA (mg / kg)} = \frac{(A - B) \times 50}{M} \quad (2)$$

where M was the weight of the sample, A, B were the absorbance of the test solution and the reagent blank, respectively.

2.7. Texture profile analysis (TPA)

The TPA was obtained following the methodology proposed by Qiu (2022) with certain modifications. The textures of the cake samples were assessed using texture analyzers (TA.XT Plus, Surrey, England). TPA was performed on cubes (15 × 15 × 15 mm) taken from the central crumb of each cake. The test speed was 2 mm/s with a strain of 60% of the original cube height and a 5 s interval between the two compression cycles, the trigger force was 2 g. The double compression test was performed with a 20 mm diameter aluminium plate. The parameters obtained from the curves were hardness, cohesiveness, chewiness, resilience, gumminess and springiness. Three cubes of each cake were measured.

2.8. Specific volume

The specific volume of each cake sample was estimated by the rapeseed displacement method (Chen et al., 2023). Measurements were conducted 2 h after baking, and the specific volume was estimated as the ratio of the cake volume to cake weight.

2.9. Sensory evaluation

The sensory evaluation of the cake was conducted in accordance with a previous study, with minor adjustments (Starowicz et al., 2018). A total of 30 untrained panelists utilized 9-point scales to assess various sensory parameters, encompassing appearance, texture, taste, flavor, color and overall acceptance.

2.10. The determination of total starch content

The determination of total starch content (TS) in the cake was conducted following the method described by Liu and Liu (2020), with certain modifications. The cakes were ground and a wet sample was prepared by adding three times the amount of water. Subsequently, 1 g of the sample was mixed with glycerol (50 wt%) to prevent aggregation, followed by the addition of 8 mL of sodium hydroxide solution (1 mol/L). The mixture was stirred at room temperature for 20 min at a speed of 180 r/min. Finally, 22 mL acetate-sodium acetate buffer (100 mol/mL, pH 4.75) was added and vortexed thoroughly before adding 8 mL of hydrochloric acid (1 mol/L), which was then vortexed at high speed for 2 min 5 mL of the mixture was aspirated and transferred to a 15 mL centrifuge tube, followed by addition of 3 mL α-amylase solution (33 mg/mL) and 3 mL phosphate buffer solution (50 mol/mL, pH 7.4). The resulting mixture was agitated in a water bath at 37 °C for 45 min (180 r/min). Upon completion of the reaction, a sample of 200 μL was extracted to determine glucose content using the GOPOD kit. The conversion coefficient from starch to glucose was determined as being equal to 0.9.

2.11. In vitro digestibility

The starch fractions were analyzed during digestion using the method described by Alvarez-Ramirez et al. (2020) with slight modifications. Specifically, cakes were ground and 1 g of the sample was accurately weighed before thorough mixing with 10 mL of acetate-sodium acetate buffer (0.25 mol/L, pH 5.2). Porcine pancreatic α-amylase (60 mg/mL), pepsin (133.6 mg/mL), and amylglucosidase (1000 mg/mL) were added in their respective quantities, and the reaction was conducted for 3 h at a speed of 180 r/min in an air bath shaker. At 0, 20, 60, 90, 120 and 180 min of digestion, a volume of 1 mL enzyme solution was withdrawn. Subsequently, the enzyme activity was terminated by adding 4 mL of anhydrous ethanol (85%) followed by centrifugation at a speed of 3500 r/min for 5 min. The resulting supernatant was analyzed for glucose content using the GOPOD kit. The quantities related to rapidly digestible starch (RDS), slowly digestible starch (SDS), resistant starch (RS) and rate of starch hydrolysis during digestion were calculated using formulas (3-6):

$$\text{RDS}(\%) = \frac{(G_{20} - G_0) \times 0.9}{TS} \times 100 \quad (3)$$

$$\text{SDS}(\%) = \frac{(G_{120} - G_{20}) \times 0.9}{TS} \times 100 \quad (4)$$

$$\text{RS}(\%) = 100\text{-RDS}(\%)\ \text{-SDS}(\%) \quad (5)$$

$$\text{Starch hydrolysis rate}(\%) = \frac{G_t \times 0.9}{TS} \times 100 \quad (6)$$

where G_0 denotes the concentration of free glucose in the biscuit; G_{20} and G_{120} represent the glucose concentrations at 20 min and 120 min of digestion, respectively; while G_t signifies the glucose concentration at time t during enzymatic hydrolysis.

2.12. X-ray diffraction (XRD)

The XRD patterns of various types of cakes were obtained using an X-ray diffractometer (D8 Advance, Bruker, Germany). The diffraction angle (2θ) range for the oleogel samples was set at 3–50°, using 0.02°/s radiation at 40 mA and 40 kV. The scanning rate was adjusted to 2θ = 12°/min. Relative crystallinity (%) of V-type crystals was determined using JADE software by calculating the percentage of diffraction peak area at 13.3°, 19.8° and 20° in relation to the total diffraction peak area.

2.13. Thermal properties

The thermal properties of the cake were determined following the methodology described by Kaur and Gill (2021) with some modifications. Heating profiles of various types of cakes were measured using a differential scanning calorimeter (Q-200, TA Instruments, USA). The preparation of cakes were dried using an Electro-thermostatic blast oven (DHG-9240A, Shanghai, China) at 50 °C for 24 h. The dried cakes crushed to powder using a grinder (02A, Guangzhou, China). A total of 8 g of cake powder was placed in the DSC crucible and then supplemented with 16 μL of distilled water. The crucible was subsequently sealed and allowed to equilibrate for 12 h. Subsequently, DSC analysis was performed with a scanning range set from 20 °C to 100 °C at a heating rate of 10 °C/min. Key parameters including initial temperature (T_o), melting temperature (T_m), end temperature (T_c) and enthalpy change (ΔH_m) associated with melting were recorded.

2.14. Fourier transform infrared (FTIR) spectroscopy

The short-range ordered structure of the cake was prepared following the method described by Alvarez-Ramirez et al. (2020) with some modifications. The FTIR spectra of various types of cakes were acquired using a Bruker Vertex 70 V FTIR spectrophotometer from Germany. Spectra were collected in the range of 4000-400 cm^{-1}, with a resolution of 1 cm^{-1} (100 scans). Omnic 9.2 software was employed for processing the infrared spectra, utilizing a half-peak width of 20 cm^{-1} and an enhancement factor of 3. Deconvolution integration within the range of 1200 cm^{-1} to 800 cm^{-1} yielded corrected heights at wavenumbers corresponding to 1047 cm^{-1}, 1022 cm^{-1} and 995 cm^{-1}.

2.15. Rheological analysis

The rheology analysis was conducted using a stress-controlled rheometer (DHR-3, Waters Instruments, USA) in accordance with a previous study (Li et al., 2022) with minor adjustments. The diameter of the aluminum plate was set at 50 mm, and the testing gap was established as 1000 μm. The strain sweep measurement was performed in a range of 0.01–100% and with an angular frequency of 1 Hz to determine the linear viscoelastic region (LVR) of all samples. Flow measurements were carried out under shear rates ranging from 0.01 to 100 s^{-1} at a temperature of 25 °C. The frequency sweep test was performed over frequencies of 0.1–40 Hz at a strain amplitude of 0.1% (within the LVR).

2.16. Statistical analysis

The experiments were conducted in triplicate, and the mean value was calculated. Statistical analysis was performed using one-way analysis of variance (ANOVA) with SPSS software, followed by Tukey's post hoc test at a significance level of $P < 0.05$. Data processing and graphing were carried out using ORIGIN software, with different letter labels indicating significant differences.

3. Results and discussion

3.1. The oxidation stability of oleogels

Olegels are highly susceptible to oxidation under aerobic conditions, so the oxidative stability of the oleogel is also an indicator for assessing the rate of oxidation of the oleogel (Yan et al., 2024). The oxidative stability of oleogels were determined by the PV and TBA value. As shown in Table 1, the PV values of Margarine, TAG-based oleogels and DAG-based oleogels were all lower than 0.04 mmol/kg. The PV value of the TAG-based oleogels was higher than those of DAG-based oleogels, and tended to decrease with increasing the GMS contents. This may be because the compact network structure of the DAG-based oleogel hampers the oil droplets from contacting with the oxygen, delaying the oxidation (Sivakanthan et al., 2024). Our previous study proved that the network structures of the DAG-based oleogels are more compact than those of the TAG-based oleogels (Chen et al., 2023). Meanwhile, the TBA values of Margarine, TAG-based oleogels and DAG-based oleogels were lower than 0.2 mg/kg, the DAG-based oleogel were much lower than those of TAG-based oleogels. These results might be due to the presence of the network structure in the DAG-based oleogel hindered the transfer of oxygen radicals, and thus inhibited the formation of TBA (Zhao et al., 2023).

3.2. TPA of cakes

Texture plays a significant role in determining consumer acceptance of cakes. Table 2 illustrates the influence of TEC-based and DEC-based oleogels on cake texture. The results demonstrated a significant increase in the hardness values of TEC cakes compared to Margarine cakes ($P < 0.05$). This can be attributed to the interaction between EC and OSA-wheat flour, which results in the formation of a more compact network structure within the cakes (Xu et al., 2023). This finding was consistent with previous research, which indicated that cakes exhibited a denser and crumblier structure, resulting in an increase in cake firmness (Alvarez-Ramirez et al., 2020). In terms of TEC-based cakes, the hardness significantly decreased with an increasing concentration of GMS, potentially due to the emulsification induced by the polar duality structure of GMS molecules (Adili, 2020). This finding was consistent with our previous results (Chen et al., 2023). The hardness of DEC-based cakes, however, exhibited lower values compared to that of TEC-based cakes as the concentration of GMS increased. This phenomenon can potentially be attributed to the emulsification caused by the polar duality structure of GMS and PDO, which could efficiently incorporate more air bubbles in batters during mixing, resulting in the lower hardness (Chen et al., 2023). Meanwhile, the incorporation of GMS and PDO might impair the negative impact of OSA-wheat flour on the softness of cakes. Punia et al. (2019) have found that the hardness of cake increases when replacing the fat to OSA-wheat flour, which may be due to reduction in air incorporation. Therefore, the findings of this study suggested that DEC-based olegels outperformed TEC-based olegels as a viable alternative to margarine in cake formulation while maintaining the original textural properties.

Table 1
PV and TBA of Margarine, TEC-based and DEC-based oleogels. TEC: peanut triacylglycerol oil/ethyl cellulose, DEC: peanut diacylglycerol oil/ethyl cellulose, GMS: glycerol monostearate.

Sample	PV(mmol/kg)	TBA (mg/kg)
Margarine	0.034 ± 0.001^{a}	0.145 ± 0.002^{f}
TEC	0.023 ± 0.001^{bc}	0.156 ± 0.002^{d}
TEC/GMS-2	0.026 ± 0.004^{b}	0.179 ± 0.001^{a}
TEC/GMS-4	0.022 ± 0.002^{c}	0.174 ± 0.002^{b}
TEC/GMS-6	0.018 ± 0.002^{d}	0.173 ± 0.001^{b}
DEC	0.022 ± 0.001^{c}	0.152 ± 0.002^{e}
DEC/GMS-2	0.022 ± 0.002^{c}	0.167 ± 0.002^{c}
DEC/GMS-4	0.017 ± 0.001^{de}	0.167 ± 0.001^{c}
DEC/GMS-6	0.014 ± 0.001^{e}	0.165 ± 0.002^{c}

Data are expressed as mean ± standard deviation (n = 3) and different letters show significant difference at the 5% level in Duncan's test ($P < 0.05$).

3.3. Specific volume of cakes

Specific volume is an essential quality indicator of baked products as it could reflects the degree of dough volume expansion and retention capacity (Tao et al., 2024). The higher the specific volume, the fluffier and better characteristics of cake. The specific volume of Margarine, TEC-based and DEC-based cakes were shown in Table 2. The specific volume of TEC and DEC cakes were lowest among TEC-based and DEC-based cakes, this might be due to the interaction between EC and OSA-wheat flour, which results in the more compact network structure in the cakes (Xu et al., 2023). Whereas the specific volume of TEC-based and DEC-based cakes increased when the GMS increased. These results might be due to the GMS could efficiently incorporate more air bubbles in batters during mixing, which was lined with TPA analysis. It worth noting that the specific volume and height of DEC-based were higher than those of TEC-based cake, which might be due to that PDO has an emulsifying ability (Chen et al., 2023). The appearances of Margarine, TEC-based and DEC-based cakes were shown in Fig. 1.

3.4. Sensory analysis of cakes

Sensory analysis is a crucial tool for comprehensively assessing the potential application of TEC-based and DEC-based cakes by understanding consumer preferences (Henning et al., 2019). In this study, the cakes are evaluated based on six criteria using a 9-point scale: appearance, texture, taste, flavor, color and overall acceptance. The sensory analysis of the TEC-based and DEC-based cakes in comparison to Margarine cakes is depicted in Fig. 2. In terms of all criteria, TEC cakes received the lowest score, while DEC-based cakes consistently exhibited higher scores compared to TEC-based cakes, respectively. Notably, DEC-based cakes exhibited minimal differences when the content of GMS was increased. These results might be associated with the texture of cakes, which could be attributed to the fact that PDO enhanced the formation of lipid-amylose complexes. However, in terms of flavor, the scores for TEC-based and DEC-based cakes were comparatively lower than those for Margarine cake, potentially attributed to the distinctive aroma associated with margarine. Among the color scores, an increase in GMS resulted in a decrease in the scores of TEC-based and DEC-based cakes compared to Margarine cakes. This observation may be

Table 2
Texture parmeters and specific volume of cakes prepared using Margarine, TEC-based and DEC-based oleogels. TEC: peanut triacylglycerol oil/ethyl cellulose, DEC: peanut diacylglycerol oil/ethyl cellulose, GMS: glycerol monostearate.

Sample	Specific volume (cm^3/g)	Hardness (g)	Cohesiveness	Chewiness (N)	Resilience	Gumminess (g)	Springiness
Margarine	20.07 ± 0.64^{e}	28056.67 ± 39.94^{c}	0.56 ± 0.04^{a}	7015.41 ± 14.80^{a}	0.27 ± 0.00^{ab}	10176.15 ± 42.95^{c}	0.54 ± 0.04^{a}
TEC	22.99 ± 0.39^{d}	33053.46 ± 23.98^{a}	0.28 ± 0.01^{f}	3467.11 ± 40.95^{e}	0.16 ± 0.00^{e}	7830.82 ± 60.93^{e}	0.37 ± 0.04^{d}
TEC/GMS-2	23.67 ± 0.62^{cd}	20588.76 ± 37.22^{f}	0.34 ± 0.01^{de}	4749.35 ± 19.17^{c}	0.27 ± 0.01^{ab}	10461.21 ± 205.95^{b}	0.42 ± 0.01^{c}
TEC/GMS-4	24.42 ± 0.58^{bc}	18606.58 ± 56.32^{g}	0.32 ± 0.00^{e}	3767.67 ± 36.84^{d}	0.26 ± 0.02^{bc}	8518.10 ± 12.25^{d}	0.45 ± 0.02^{bc}
TEC/GMS-6	25.16 ± 0.77^{ab}	11083.52 ± 64.64^{h}	0.44 ± 0.05^{b}	6736.28 ± 30.84^{b}	0.29 ± 0.01^{a}	13917.88 ± 47.25^{a}	0.48 ± 0.01^{b}
DEC	23.20 ± 0.55^{cd}	32468.56 ± 245.44^{b}	0.24 ± 0.00^{g}	1635.7 ± 36.49^{h}	0.22 ± 0.01^{d}	4538.2 ± 23.46^{g}	0.38 ± 0.02^{d}
DEC/GMS-2	23.96 ± 1.45^{cd}	23289.14 ± 316.67^{d}	0.28 ± 0.00^{f}	2572.97 ± 51.77^{g}	0.15 ± 0.00^{e}	5715.23 ± 64.06^{f}	0.44 ± 0.01^{bc}
DEC/GMS-4	25.14 ± 0.76^{ab}	21500.60 ± 384.19^{e}	0.38 ± 0.00^{cd}	1004.06 ± 23.83^{i}	0.25 ± 0.01^{c}	3021.57 ± 14.73^{h}	0.46 ± 0.01^{bc}
DEC/GMS-6	26.05 ± 0.30^{a}	20500.80 ± 349.14^{f}	0.40 ± 0.01^{bc}	3008.54 ± 18.77^{f}	0.26 ± 0.01^{bc}	7873.18 ± 44.55^{e}	0.44 ± 0.01^{bc}

Data are expressed as mean ± standard deviation (n = 3) and different letters show significant difference at the 5% level in Duncan's test ($P < 0.05$).

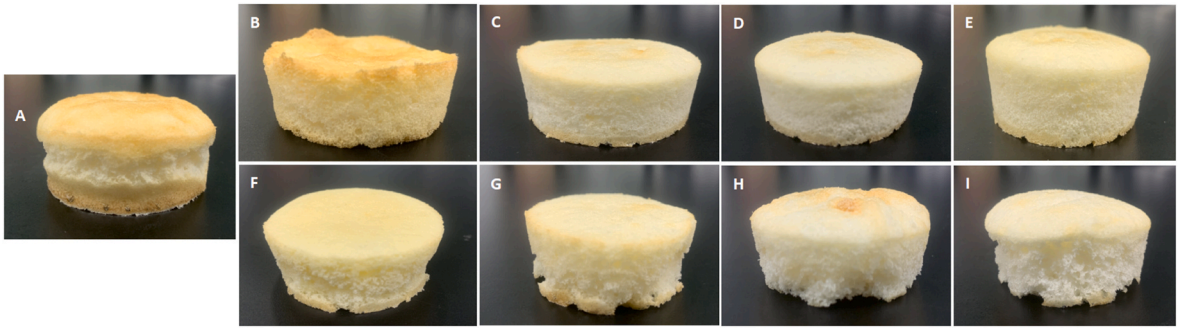

Fig. 1. The visual appearance of cakes prepared by Margarine, TAG-based and DAG-based oleogels. (A) Margarine cake, (B) TEC cake, (C) TEC/GMS-2 cake, (D)TEC/GMS-4 cake, (E) TEC/GMS-6 cake, (F) DEC cake, (G) DEC/GMS-2 cake, (H) DEC/GMS-4 cake, and (I) DEC/GMS-6 cake. TEC: peanut triacylglycerol oil/ethyl cellulose, DEC: peanut diacylglycerol oil/ethyl cellulose, GMS: glycerol monostearate.

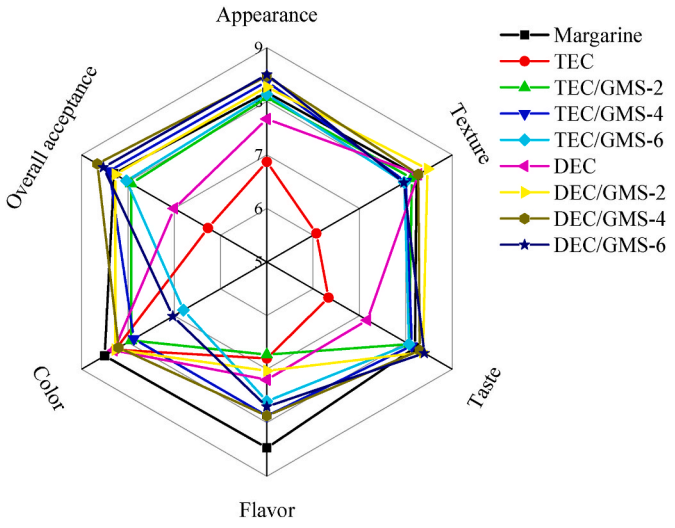

Fig. 2. Sensory evaluation of cakes prepared using Margarine, TEC-based and DEC-based cakes.TEC: peanut triacylglycerol oil/ethyl cellulose, DEC: peanut diacylglycerol oil/ethyl cellulose, GMS: glycerol monostearate.

attributed to the reduced EC content, which could potentially mitigate Maillard reaction at higher temperatures. A similar study published by Adili (2020) also reported that EC can induce the Maillard reaction at high temperatures. The overall acceptance of DEC/GMS-4 oleogels was relatively high, as evidenced by sensory scores exceeding 8.66 among them.

3.5. The effect of oleogel on the digestibility of cakes

The starch in TEC-based and DEC-based cakes can be categorized into three distinct types, namely rapidly digestible starch (RDS), slowly digestible starch (SDS) and resistant starch (RS) (Zhang et al., 2023; G. Zhang et al., 2023).The consumption of rapidly digestible starch (RDS) leads to an increase of postprandial glycemic levels (Xu et al., 2023), thus playing a pivotal role in the pathogenesis of type II diabetes. The consumption of SDS and RS contributes to maintaining postprandial glycemic levels for an extended period (Xu et al., 2023). Therefore, enhancing the concentration of SDS and RS is a preferable approach to regulate blood glucose levels and promote gastrointestinal health in humans (Liang et al., 2023).

The in vitro digestibility of cakes with different formulations is summarized in Table 3. Table 3 illustrated that the Margarine cakes contained 40.00%, 38.38%, and 21.62% of RDS, SDS, and RS, respectively. Among all cakes, the RS content of TEC-based and DEC-based cakes was higher than that of Margarine cakes. For TEC-based cakes, when the GMS concentration was 0%, the TEC/GMS-2 and TEC/GMS-4 cakes resulted in a significant reduction in RS content of 8.65% and

Table 3
Rapidly digestible starch (RDS), slowly digestible starch (SDS) and resistant starch (RS) of Margarine, TEC-based and DEC-based cakes. TEC: peanut triacylglycerol oil/ethyl cellulose,DEC: peanut diacylglycerol oil/ethyl cellulose, GMS: glycerol monostearate.

Sample	RDS (%)	SDS (%)	RS (%)
Margarine	40.00 ± 1.82^{b}	38.38 ± 1.50^{a}	21.62 ± 0.43^{e}
TEC	35.65 ± 1.32^{cd}	26.12 ± 1.75^{cd}	38.22 ± 3.07^{b}
TEC/GMS-2	45.67 ± 1.98^{a}	24.76 ± 1.42^{d}	29.57 ± 3.04^{d}
TEC/GMS-4	34.42 ± 2.09^{cd}	32.15 ± 1.15^{b}	33.43 ± 2.99^{c}
TEC/GMS-6	33.27 ± 0.45^{d}	28.06 ± 1.48^{c}	38.67 ± 1.93^{b}
DEC	46.80 ± 1.41^{a}	12.28 ± 0.67^{g}	40.92 ± 1.02^{ab}
DEC/GMS-2	41.45 ± 1.28^{b}	15.74 ± 0.98^{f}	42.80 ± 2.23^{a}
DEC/GMS-4	36.16 ± 1.91^{c}	20.98 ± 1.13^{e}	42.86 ± 1.23^{a}
DEC/GMS-6	18.64 ± 0.62^{e}	39.89 ± 1.46^{a}	41.47 ± 1.07^{ab}

Data are expressed as mean ± standard deviation (n = 3) and different letters show significant difference at the 5% level in Duncan' s test ($P < 0.05$).

4.79%, respectively, compared to that of TEC cakes. This observation can be attributed to the formation of a compact network formed by EC and OSA-wheat flour, which potentially hindered α-amylase's accessibility to starch. The findings of this study were consistent with those reported by Zhang et al. (2023), who found that compact network would result in an increase in RS content. When the concentration of GMS was increased from 2% to 6%, an increase in RS content was observed, indicating an enhanced formation of lipid-amylose complexes. The formation mechanism of lipid-amylose complexes and their resistance to amylase digestion are illustrated in Fig. 3 through a schematic diagram. However, the RDS content exhibited no significant variation across different levels of GMS but remained lower than that observed in Margarine cakes. This observation suggested that TEC-based oleogels exerted minimal influence on cake digestibility.

The RS contents in DEC-based cakes showed no significant difference when the concentration of GMS increased, consistently surpassing those observed in TEC-based cakes. This observation suggested that DEC-based oleogels had a greater influence on cake digestibility compared to TEC-based oleogels. This phenomenon may be attributed to the synergistic effect of PDO and GMS on the formation of lipid-amylose complexes (Feng et al., 2024; Kawai et al., 2012). The noteworthy observation was that an increased GMS content resulted in a gradual reduction in RDS content. When the GMS concentration reached 6%, the RDS content decreased of 21.36% compared to Margarine cakes. Therefore, these results suggested that the incoprporaiton of DEC-based olegels in cake formulations resulted in a reduction in starch digestibility. To further validate the formation of lipid-amylose complexes, comprehensive analyses were performed, including X-ray diffraction (XRD), differential scanning calorimetry (DSC), Fourier-transform infrared spectroscopy (FTIR), and rheological measurements.

3.6. The underlying mechanism of oleogel on the digestibility of cakes

3.6.1. Crystallization of cakes

The interaction between amylose in OSA-wheat flour and lipids in TEC-based and DEC-based oleogels can be analyzed by XRD to determine the crystallization of cakes (Ahmed et al., 2019). As depicted in Fig. 4, the TEC-based and DEC-based cakes exhibited diffraction peaks at approximately 13.3°, 19.8°, and 20° compared to Margarine cakes, indicating the formation of lipid-amylose complexes. The present findings were consistent with those reported by Ahmed et al. (2019), who demonstrated that the lipid-amylose complexes were characterized by diffraction peaks at approximately 13.3°, 19.8°, and 20°.

The relative crystallinity of lipid-amylose complexes is presented in Fig. 4. The Margarine cakes were found to have a relative crystallinity of 0%, indicating the absence of lipid-amylose complexes in these cakes. It is worth noting that when the concentration of GMS was 0%, the relative crystallinity of TEC cake was also found to be 0%, while the relative crystallinity of DEC cake exhibited 8.18%. This observation could potentially be attributed to the formation of lipid-amylose complexes in DEC cake resulting from the interaction between PDO and OSA-wheat flour (Liu et al., 2022). For TEC-based cakes, an increase in GMS content resulted in a gradual improvement in the relative crystallinity of lipid-amylose complexes, ranging from 11.56% to 32.81%. While, for DEC-based cakes, an increase in GMS content from 0% to 6% resulted in a wider relative crystallinity, ranging from 19.09% to 44.41%, surpassing that observed for TEC-based cakes. These findings suggested that the formation of lipid-amylose complexes in TEC-based cake might be caused by the interaction between GMS and OSA-wheat flour, while

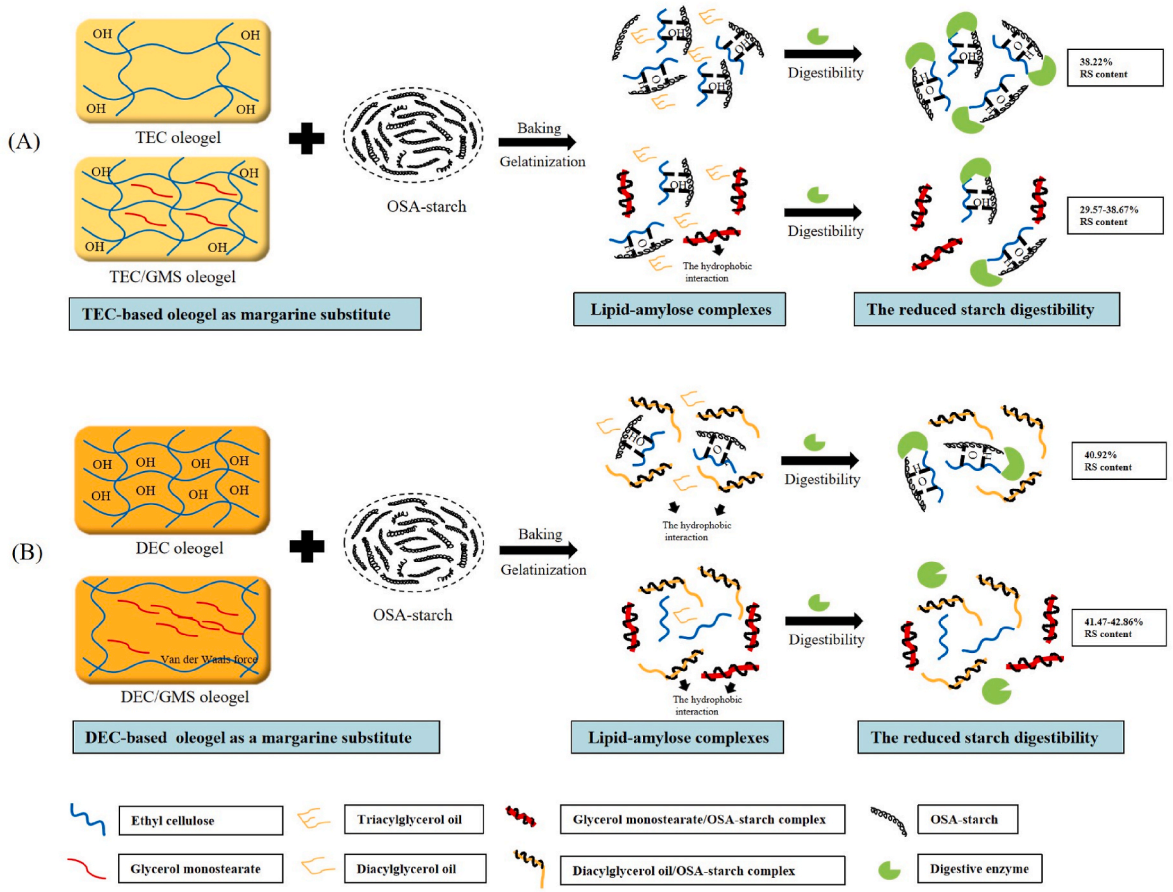

Fig. 3. The formation mechanism of lipid-amylose complexes and their resistance to amylase digestion in TEC-based (A) and DEC-based (B) cakes. TEC: peanut triacylglycerol oil/ethyl cellulose, DEC: peanut diacylglycerol oil/ethyl cellulose, GMS: glycerol monostearate, OSA: octenyl succinic anhydride.

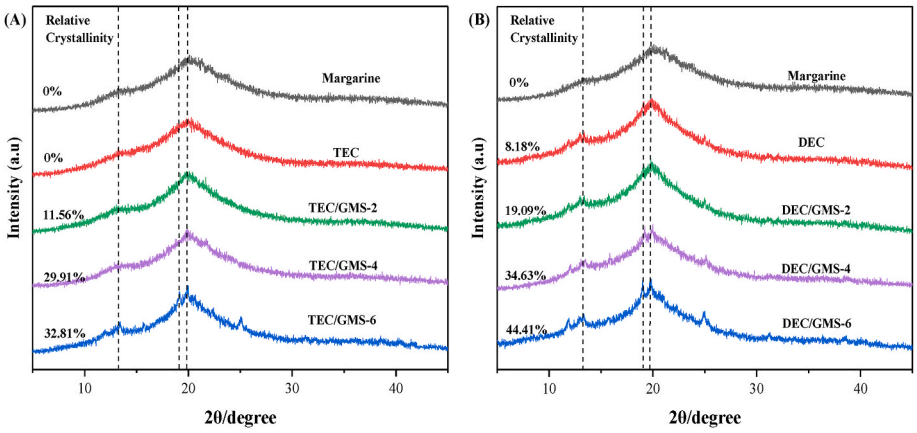

Fig. 4. XRD patterns of Margarine, TEC-based (A) and DEC-based (B) cakes. TEC: peanut triacylglycerol oil/ethyl cellulose, DEC: peanut diacylglycerol oil/ethyl cellulose, GMS: glycerol monostearate.

the presence of PDO in DEC-based oleogels might facilitate these formation of the complexes in DEC-based cakes. Zheng et al. (2023) found similar results indicating that polar lipids such as fatty acids, glycerol monostearate, and diglycerides have a higher tendency to form complexes with amylose. Kawai et al. (2012) demonstrated that an increase in crystallinity resulted in a reduced water diffusion rate and enzyme sensitivity, leading to a decrease in starch digestion rate and an elevation in SDS and RS content. Therefore, we hypothesized that the elevated levels of GMS may contribute to the decreased starch digestibility in TEC-based and DEC-based cakes.

3.6.2. Thermal properties of cakes

The gelatinization properties of starch in different cake formulations were investigated through DSC analysis, as reported by Ding et al. (2021). The parameters such as the initial temperature (T_o), melting temperature (T_m), final temperature (T_c), and enthalpy change (ΔH_m) were utilized to evaluate the gelatinization characteristics of starch in cakes. The starch gelatinization behavior of margarine, TEC-based and DEC-based cakes with different GMS contents is presented in Table 4.

The ΔH_m value serves as a quantitative indicator of complexes, reflecting their degree of crystallinity (Kawai et al., 2012). The ΔH_m values of TEC-based cakes exhibited an increasing trend with a higher content of GMS, which increased from 128.10 °C to 769.40 °C compared to that observed in TEC cakes. These results could be attributed to the fact that the formation of lipid-amylose complexes between GMS in TEC-based oleogel and amylose present in OSA-wheat flour. These results were consistent with those reported by Kawai et al. (2012), who observed that the higher ΔH_m value indicated potential complexes formation between amylose and GMS during the hydrolysis of gelatinized starch. Henning et al. (2019) also found that starches with a higher content of lipid-amylose complexes exhibited an enhanced ΔH_m during gelatinization. However, there were no significant differences ($P > 0.05$) in the ΔH_m values of DEC-based cakes containing 0–6% GMS; nevertheless, these values exceeded those of Margarine cakes by approximately 300 J/g. The results of this study suggested that the formation of lipid-amylose complexes was primarily driven by hydrophobic interactions between the hydrophobic core of the amylose helix in OSA-wheat flour and the hydrophobic moieties present in PDO, rather than GMS. These results may be attributed to the partial substitution of hydroxyl groups of starch granules in wheat flour with hydrophobic OSA groups, which endows raw starch with both hydrophilic and hydrophobic properties (Romero Hernández, Gutiérrez, Tovar and Bello-Pérez, 2023; Wei et al., 2023). The present findings were consistent with the previous research conducted by Wang et al. (2021), which proposed that the interaction between palm diacylglycerol and OSA-wheat flour through hydrophobic interactions. Feng et al. (2024) also utilized molecular dynamics simulations to demonstrate that amylose tended to form V6-type helices around dimyristoyl- and distearoyl-glycerol through hydrophobic interactions.

Table 4
Differential scanning calorimetry (DSC) thermograms of the Margarine, TEC-based and DEC-based cakes.TEC: peanut triacylglycerol oil/ethyl cellulose, DEC: peanut diacylglycerol oil/ethyl cellulose, GMS: glycerol monostearate, T_o: initial temperature, T_m: melting temperature, T_c: final temperature, ΔH_m: enthalpy change.

Sample	T_o (°C)	T_m (°C)	T_c (°C)	ΔH_m (J/g)
Margarine	54.8	70.6	76.5	249.7
TEC	61.6	69.3	73.7	128.1
TEC/GMS-2	45.6	68.4	77.6	456.3
TEC/GMS-4	22.1	68.9	75.1	596.9
TEC/GMS-6	27.4	68.7	74.3	769.4
DEC	46.7	70.4	76.8	564.1
DEC/GMS-2	37.7	69.0	75.1	544.6
DEC/GMS-4	23.3	68.8	75.1	583.0
DEC/GMS-6	30.1	70.4	76.6	551.9

3.6.3. FTIR spectra of cakes

The molecular interactions between amylose in OSA-wheat flour and lipids in Margarine cakes, TEC-based cakes, and DEC-based cakes were investigated using FTIR. The FTIR spectra of cakes are depicted in Fig. 5 (A, B). The prominent peak observed between 3200 and 3500 cm^{-1} corresponded to the N–H bending vibrations of gluten molecules (Cheng et al., 2022). The absorption peaks observed at 2854 cm^{-1} and 2931 cm^{-1} were attributed to the vibrations of C–H bonds in lipids (Liang et al., 2023). The absorption peak observed at 1743 cm^{-1} was ascribed to the vibration of the C═O bond (Althawab et al., 2023). The fingerprint region (1200–800 cm^{-1}) and the peak intensity ratio of starch molecules are illustrated in Fig. 6 (A-D), where the crystalline domain is characterized by a peak at 1047 cm^{-1}, the amorphous domain is characterized by a peak at 1022 cm^{-1}, and the intermolecular hydrogen bond strength between starch molecules is indicated by a peak at 998 cm^{-1}. The absorption ratio at 1047 cm^{-1} and 1022 cm^{-1} ($R_{1047/1022}$) is employed to characterize the short-range ordered structure of starch. A higher ratio indicates a stronger short-range ordered structure (Wang et al., 2015), resulting in enhanced resistance to amylase digestion (Tang et al., 2021; Yan et al., 2020). The absorption ratio at 1022 cm^{-1} and 998 cm^{-1} ($R_{1022/998}$) reflects the strength of hydrogen bond forces, with a lower intensity indicating stronger intermolecular hydrogen bond forces among starch molecules (Wang et al., 2022).

Among TEC-based cakes, the $R_{1047/1022}$ and $R_{1022/998}$ values of TEC cakes were found to be the highest and lowest, measuring 1.25 and 0.13, respectively, as depicted in Fig. 6 (C). This observation suggested a more

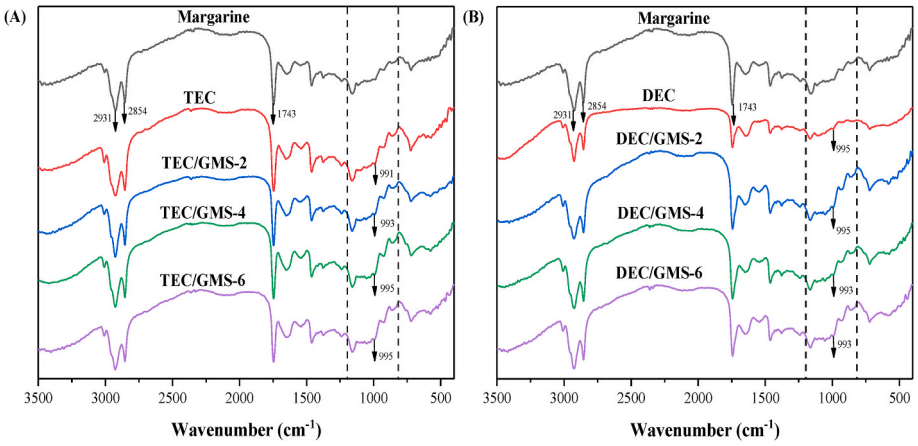

Fig. 5. Fourier transform infrared spectra of Margarine, TEC-based (A) and DEC-based (B) cakes. TEC: peanut triacylglycerol oil/ethyl cellulose, DEC: peanut diacylglycerol oil/ethyl cellulose, GMS: glycerol monostearate.

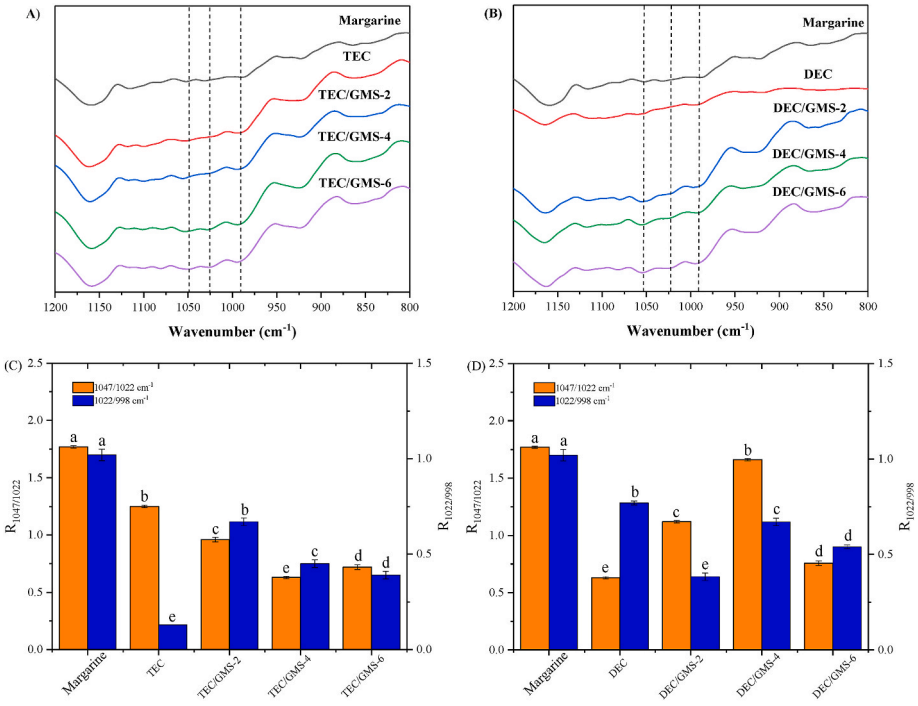

Fig. 6. The fingerprint region (1200-800 cm^{-1}) and peak intensity ratio of Margarine, TEC-based (A, C) and DEC-based (B, D) cakes. TEC: peanut triacylglycerol oil/ethyl cellulose, DEC: peanut diacylglycerol oil/ethyl cellulose, GMS: glycerol monostearate. $R_{1047/1022}$ is intensity ratio of the bands at 1047 and 1022 cm^{-1} , $R_{1022/998}$ is intensity ratio of the bands at 1022 and 998 cm^{-1}.

robust short-range ordered structure and stronger intermolecular hydrogen interactions within the TEC cake. These findings can be attributed to the formation of hydrogen bonds between the hydroxyl groups of starch molecules in OSA-wheat flour and those of EC, which was consistent with a previous study (Xu et al., 2023), where the interaction between starch molecular chains of OSA-wheat flour and hydroxyl groups of cellulose nanocrystals resulted in locally ordered aggregates. The peak at 991 cm^{-1} was attributed to the hydrogen bond formed by hydroxyl group of the glucose unit in starch (Fig. 5A). With an increase in the content of EC, a slight red shift was observed at 991 cm^{-1}, indicating the disruption of hydrogen bonds within the glucose units and the formation of new hydrogen bonds with EC. Similarly, the study by Xu et al. (2023) also reported a red shift of peak at 988 cm^{-1} with an increased concentration of nanocrystalline cellulose. However, for DEC cake, The $R_{1047/1022}$ and $R_{1022/998}$ values were found to be the lowest and highest, respectively (Fig. 6D). The observed outcomes may be attributed to the formation of lipid-amylose complexes between OSA-wheat flour and PDO, primarily achieved through hydrophobic interactions that occurred between the hydrophobic core of the amylose helix and the hydrophobic groups of PDO (Wang et al., 2021). Therefore, the main force driving the structure of the DEC cake was hydrophobic interactions between lipid-amylose complexes, which resulted in a weakened short-range ordered structure and reduced intermolecular hydrogen bonding (Chen et al., 2023).

When the content of GMS increased from 2% to 6%, a slight decrease in the $R_{1047/1022}$ and $R_{1022/998}$ values was observed in the TEC-based cake, resulting in a decrease of approximately 25.00% and 41.79%, respectively. The results indicated a decrease in the strength of the short-range ordered structure and an increase in the intermolecular hydrogen interactions, possibly attributed to a higher degree of hydrogen

interaction between EC and OSA-wheat flour chains compared to the hydrophobic interaction between GMS and OSA-wheat flour chains (Xu et al., 2023). The short-range ordered structure in DEC-based cakes, however, exhibited enhanced strength as the GMS content increased to 4%. The $R_{1047/1022}$ value of DEC/GMS-4 cake exhibited a significantly higher magnitude of 62.05% compared to that observed in the DEC cake, potentially indicating the formation of lipid-amylose complexes induced by both PDO and GMS (Feng et al., 2024; Kawai et al., 2012). The previous study conducted by Wang et al. (2015) demonstrated that the presence of enhanced hydrogen bonding forces and a short-range ordered structure could potentially contribute to a reduction in starch digestibility. These findings indicated that the DEC-based cakes exhibited significantly stronger hydrogen bonding forces and a more pronounced short-range ordered structure, potentially resulting in its reduced starch digestibility.

3.6.4. *Rheological properties of cake batters*

To investigate the influence of TEC-based and DEC-based oleogels on the continuous phase of starch in cake batters, viscoelastic profiles and dynamic rheological measurements were conducted (Chen et al., 2022). The results presented in Fig. 7 (A, B) demonstrated that the apparent viscosity of TEC-based and DEC-based cakes exhibited shear thinning behavior with increasing shear rate, which was a characteristic feature of pseudoplastic non-Newtonian fluids (Chang et al., 2023). The viscoelasticity of TEC-based cakes was enhanced with the increased GMS, which could be attributed to the potential formation of hydrogen bonds between starch and EC, resulting in an enhancement in viscoelasticity. This observation was consistent with a previous study by Xu et al. (2023), which demonstrated that the hydrophilic characteristics of cellulose nanocrystal can enhance the hydrogen bonding between starch molecules in OSA-wheat flour, thereby promoting viscoelasticity of OSA-wheat flour. However, the viscoelasticity of DEC/GMS-4 cakes was significantly lower than that of other DEC-based cakes. These results might be attributed to the fact that the formation of lipid-amylose complexes primarily relied on hydrophobic interactions between the hydrophobic core of the amylose helix of OSA-wheat flour and the hydrophobic moieties of GMS (Romero Hernández et al., 2023; Wei et al., 2023), rather than hydrogen bonding. The OSA modification might also lead to a decrease in viscoelasticity of starch. This observation aligns with a previous investigation conducted by Wang et al. (2024), which

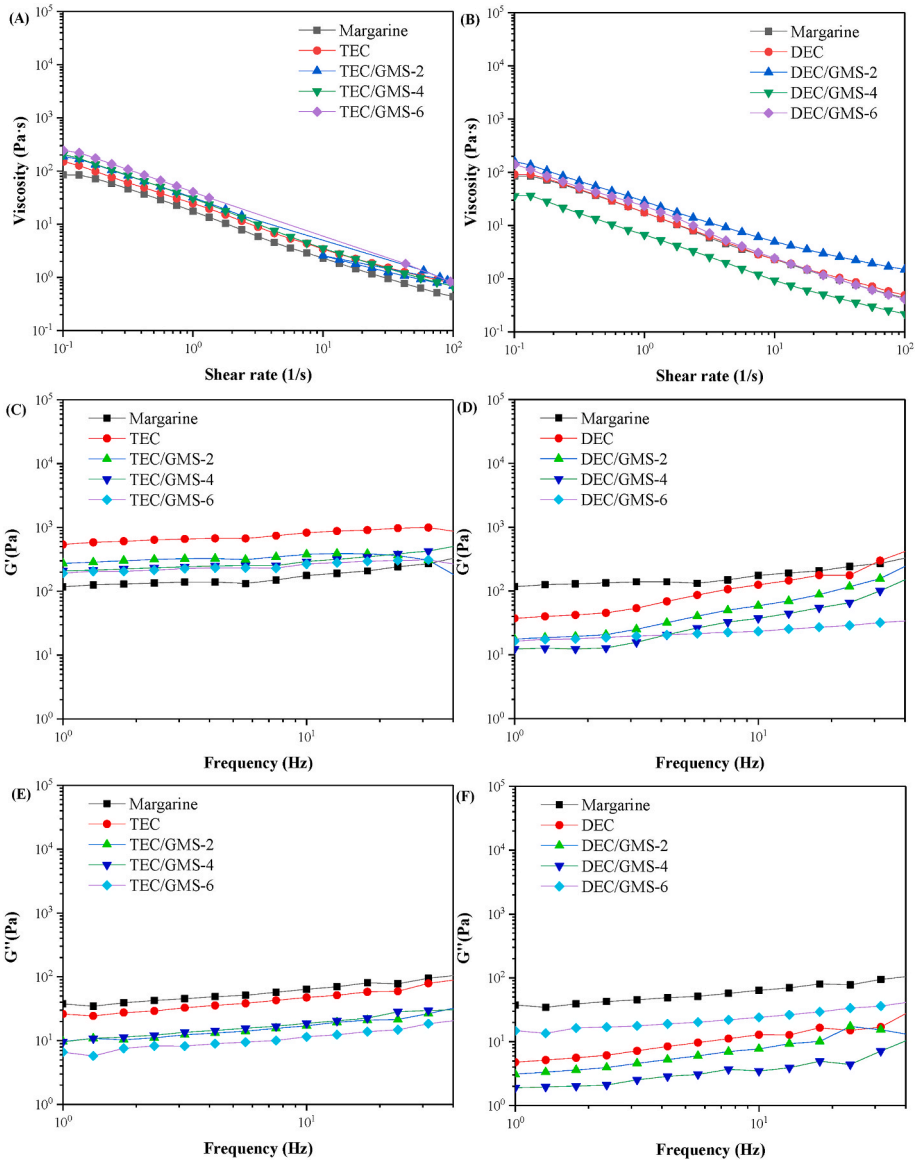

Fig. 7. The viscoelastic and dynamic rheological properties of the Margarine, TEC-based and DEC-based cakes. TEC: peanut triacylglycerol oil/ethyl cellulose, DEC: peanut diacylglycerol oil/ethyl cellulose, GMS: glycerol monostearate. G′ denotes storage modulus, G″ represents loss modulus.

demonstrated that OSA modification could result in a significant reduction in the viscoelasticity of highland barley starch.

The elasticity of cakes can be characterized by the storage modulus (G′) and the loss modulus (G″). The storage modulus (G′) is determined by measuring the energy stored in cakes during shearing, which indicates their elastic behavior. In contrast, the loss modulus (G″) represents the energy dissipated and lost by the cakes during shearing, reflecting their viscous behavior accurately (Chang et al., 2023). The results depicted in Fig. 7 C–F indicated that G′ was significantly higher ($P < 0.05$) than G″ in both TEC-based and DEC-based cakes, suggesting the presence of a characteristic weak gel network structure. This observation demonstrated that the viscoelastic behavior solid-like characteristics (Chen et al., 2022). For TEC cake, the addition of EC resulted in an increase in both G'and G″, potentially due to the formation of a more compact three-dimensional structure through cross-linking between EC molecules. Previous studies have indicated that cellulose nanocrystal can establish a stable polymer network (Chen et al., 2022). However, the increased GMS content led to a decrease in the G'value of TEC-based and DEC-based cakes, potentially due to the high hydrophobicity of GMS. These results were consistent with those of Chen et al. (2022), who found that the hydrophobic nature of stearic acid could result in a lower G'value. When the GMS content was increased, the G'value of DEC-based cakes exhibited a slightly lower compared to that of TEC-based cakes. This finding was consistent with the FTIR results, suggesting the dominant force within the DEC cake primarily arose from hydrophobic interactions of lipid-amylose complexes. The reduction in G′ may also be attributed to the ability of OSA modification. This finding was consistent with a previous study conducted by Wang et al. (2024), which demonstrated a significant decrease in the viscoelasticity and G′ of OSA-modified highland barley starch.

4. Conclusion

The present investigation has demonstrated that the DEC-based cakes could reduce starch digestibility compared to cakes containing commercial margarine. The in vitro digestibility analysis revealed that DEC/GMS cakes exhibited a significant 21.36% reduction in RDS content and a 26.36% increase in SDS and RS values compared to Margarine cakes, which can be attributed to their enhanced crystallinity of lipid-amylose complexes. The FTIR analysis revealed that the addition of GMS and PDO could facilitate the formation of lipid-amylose complexes, which might be attributed to the higher hydrophobicity of OSA-wheat flour. DEC/GMS cakes exhibited greater gelatinization enthalpy change, which might be due to lipid-amylose complexes maintaining a higher degree of crystallinity. Sensory analysis, specific volume and TPA of cakes indicated that DEC-based olegels outperformed TEC-based olegels as a viable alternative to margarine due to their softer texture. Therefore, these results demonstrate that the utilization of DEC-based oleogel is a feasible alternative for replacing margarine in cake formulations.

CRediT authorship contribution statement

Xiaohan Chen: Investigation, Writing – original draft, Formal analysis. **Dongming Lan:** Writing – review & editing. **Daoming Li:** Writing – review & editing. **Weifei Wang:** Writing – review & editing, Supervision, Funding acquisition. **Yonghua Wang:** Writing – review & editing.

Declaration of competing interest

The authors declare that they have no known competing financial interests or personal relationships that could have appeared to influence the work reported in this paper.

Data availability

Data will be made available on request.

Acknowledgements

Funding: This work was supported by the China Agriculture Research System [grant numbers CARS-18-ZJ0503].

References

Adili, 2020. Development and characterization of reinforced ethyl cellulose based oleogel with adipic acid: its application in cake and beef burger. Lwt 126. https://doi.org/10.1016/j.lwt.2020.109277.

Ahmed, M.I., Xua, X., Sulieman, A.A., Mahdi, A.A., Na, Y., 2019. Effects of fermentation time on rheological and physicochemical characteristics of koreeb (Dactyloctenium aegyptium) seed flour dough and kisra bread. J. Food Meas. Char. 13 (3), 2136–2146. https://doi.org/10.1007/s11694-019-00134-3.

Aliasl Khiabani, A., Tabibiazar, M., Roufegarinejad, L., Hamishehkar, H., Alizadeh, A., 2020. Preparation and characterization of carnauba wax/adipic acid oleogel: a new reinforced oleogel for application in cake and beef burger. Food Chem. 333, 127446 https://doi.org/10.1016/j.foodchem.2020.127446.

Althawab, S.A., Amoako, D.B., Annor, G.A., Awika, J.M., 2023. Stability of starch-proanthocyanidin complexes to in-vitro amylase digestion after hydrothermal processing. Food Chem. 421, 136182 https://doi.org/10.1016/j.foodchem.2023.136182.

Alvarez-Ramirez, J., Vernon-Carter, E.J., Carrera-Tarela, Y., Garcia, A., Roldan-Cruz, C., 2020. Effects of candelilla wax/canola oil oleogel on the rheology, texture, thermal properties and in vitro starch digestibility of wheat sponge cake bread. Lwt 130. https://doi.org/10.1016/j.lwt.2020.109701.

Barragán-Martínez, L.P., Román-Guerrero, A., Vernon-Carter, E.J., Alvarez-Ramirez, J., 2022. Impact of fat replacement by a hybrid gel (canola oil/candelilla wax oleogel and gelatinized corn starch hydrogel) on dough viscoelasticity, color, texture, structure, and starch digestibility of sugar-snap cookies. Int. J. Gastron. Food Sci. 29 https://doi.org/10.1016/j.ijgfs.2022.100563.

Cervantes-Ramirez, J.E., Cabrera-Ramirez, A.H., Morales-Sanchez, E., Rodriguez-Garcia, M.E., Reyes-Vega, M.L., Ramirez-Jimenez, A.K., et al., 2020. Amylose-lipid complex formation from extruded maize starch mixed with fatty acids. Carbohydr. Polym. 246, 116555 https://doi.org/10.1016/j.carbpol.2020.116555.

Chang, L., Zhao, N., Jiang, F., Ji, X., Feng, B., Liang, J., et al., 2023. Structure, physicochemical, functional and in vitro digestibility properties of non-waxy and waxy proso millet starches. Int. J. Biol. Macromol. 224, 594–603. https://doi.org/10.1016/j.ijbiomac.2022.10.149.

Chen, J., Cai, H., Yang, S., Zhang, M., Wang, J., Chen, Z., 2022. The formation of starch-lipid complexes in instant rice noodles incorporated with different fatty acids: effect on the structure, in vitro enzymatic digestibility and retrogradation properties during storage. Food Res. Int. 162 (Pt A), 111933 https://doi.org/10.1016/j.foodres.2022.111933.

Chen, X., Ding, S., Chen, Y., Lan, D., Wang, W., Wang, Y., 2023. Assessing the effectiveness of peanut diacylglycerol oil-ethylcellulose/monoglyceride-based oleogel in sponge cake as a margarine replacer. Food Biosci. 55 https://doi.org/10.1016/j.fbio.2023.102959.

Cheng, Z., Li, J., Qiao, D., Wang, L., Zhao, S., Zhang, B., 2022. Microwave reheating enriches resistant starch in cold-chain cooked rice: a view of structural alterations during digestion. Int. J. Biol. Macromol. 208, 80–87. https://doi.org/10.1016/j.ijbiomac.2022.03.034.

Ding, L., Xie, Z., Fu, X., Wang, Z., Huang, Q., Zhang, B., 2021. Structural and in vitro starch digestion properties of potato parenchyma cells: effects of gelatinization degree. Food Hydrocolloids 113. https://doi.org/10.1016/j.foodhyd.2020.106464.

Feng, Y., Junejo, S.A., Zhang, B., Fu, X., Huang, Q., 2024. Amylose complexation with diacylglycerols involves multiple intermolecular interaction mechanisms. Food Hydrocolloids 146. https://doi.org/10.1016/j.foodhyd.2023.109251.

Garcia-Ortega, M.L., Toro-Vazquez, J.F., Ghosh, S., 2021. Development and characterization of structured water-in-oil emulsions with ethyl cellulose oleogels. Food Res. Int. 150 (Pt B), 110763 https://doi.org/10.1016/j.foodres.2021.110763.

Henning, F.G., Schnitzler, E., Demiate, I.M., Lacerda, L.G., Ito, V.C., Malucelli, L.C., da Silva Carvalho Filho, M.A., 2019. Fortified rice starches: the role of hydrothermal treatments in zinc entrapment. Starch - Stärke 71 (1–2). https://doi.org/10.1002/star.201800130.

Kaur, H., Gill, B.S., 2021. Changes in physicochemical, nutritional characteristics and ATR-FTIR molecular interactions of cereal grains during germination. J. Food Sci. Technol. 58 (6), 2313–2324. https://doi.org/10.1007/s13197-020-04742-6.

Kawai, K., Takato, S., Sasaki, T., Kajiwara, K., 2012. Complex formation, thermal properties, and in-vitro digestibility of gelatinized potato starch–fatty acid mixtures. Food Hydrocolloids 27 (1), 228–234. https://doi.org/10.1016/j.foodhyd.2011.07.003.

Lei, M., Jiang, F.-C., Cai, J., Hu, S., Zhou, R., Liu, G., et al., 2018. Facile microencapsulation of olive oil in porous starch granules: fabrication, characterization, and oxidative stability. Int. J. Biol. Macromol. 111, 755–761.

Li, J., Shen, M., Xiao, W., Li, Y., Pan, W., Xie, J., 2023. Regulating the physicochemical and structural properties of different starches by complexation with tea polyphenols. Food Hydrocolloids 142. https://doi.org/10.1016/j.foodhyd.2023.108836.

Li, S., Zhu, L., Wu, G., Jin, Q., Wang, X., Zhang, H., 2022. Relationship between the microstructure and physical properties of emulsifier based oleogels and cookies quality. Food Chem. 377, 131966 https://doi.org/10.1016/j.foodchem.2021.131966.

Liang, W., Ding, L., Guo, K., Liu, Y., Wen, X., Kirkensgaard, J.J.K., et al., 2023. The relationship between starch structure and digestibility by time-course digestion of amylopectin-only and amylose-only barley starches. Food Hydrocolloids 139. https://doi.org/10.1016/j.foodhyd.2023.108491.

Liu, K., Liu, Q., 2020. Enzymatic determination of total starch and degree of starch gelatinization in various products. Food Hydrocolloids 103. https://doi.org/10.1016/j.foodhyd.2019.105639.

Liu, Q., Wang, Y., Yang, Y., Yu, X., Xu, L., Jiao, A., Jin, Z., 2023. Structure, physicochemical properties and in vitro digestibility of extruded starch-lauric acid complexes with different amylose contents. Food Hydrocolloids 136. https://doi.org/10.1016/j.foodhyd.2022.108239.

Liu, S., Sun, S., Chen, W., Jia, R., Zheng, B., Guo, Z., 2022. Structural, physicochemical properties, and digestibility of lotus seed starch-conjugated linoleic acid complexes. Int. J. Biol. Macromol. 214, 601–609. https://doi.org/10.1016/j.ijbiomac.2022.06.143.

Punia, S., Siroha, A.K., Sandhu, K.S., Kaur, M., 2019. Rheological and pasting behavior of OSA modified mungbean starches and its utilization in cake formulation as fat replacer. Int. J. Biol. Macromol. 128, 230–236. https://doi.org/10.1016/j.ijbiomac.2019.01.107.

Qiu, 2022. Stabilisation of oleofoams by lauric acid and its glycerol esters. Food Chem. 386, 132776 https://doi.org/10.1016/j.foodchem.2022.132776.

Rodriguez-Hernandez, 2021. Rheological properties of ethyl cellulose-monoglyceride-candelilla wax oleogel vis-a-vis edible shortenings. Carbohydrate Polymers 252, 117171. https://doi.org/10.1016/j.carbpol.2020.117171.

Romero Hernández, H.A., Gutiérrez, T.J., Tovar, J., Bello-Pérez, L.A., 2023. Complexation of octenyl succinic anhydride-esterified corn starch/polyphenol-rich Roselle (Hibiscus sabdariffa L.) extract: structural and digestibility features. Food Hydrocolloids 145. https://doi.org/10.1016/j.foodhyd.2023.109125.

Roufegarinejad, L., Dehghani, S., Bakhshi, S., Toker, O.S., Pirouzian, H.R., Khiabani, A. H., 2023. Oleogelation of sunflower-linseed oils with carnauba wax as an innovative strategy for shortening substitution in cakes. Food Chem. https://doi.org/10.1016/j.foodchem.2023.137745.

Rupp, T.M., Cramer, H., 2022. CMC and regulatory aspects of oligonucleotide therapeutics. In: RNA Therapeutics. Elsevier, pp. 263–320.

Sivakanthan, S., Fawzia, S., Mundree, S., Madhujith, T., Karim, A., 2024. Investigation of the influence of minor components and fatty acid profile of oil on properties of beeswax and stearic acid-based oleogels. Food Res. Int. 184, 114213 https://doi.org/10.1016/j.foodres.2024.114213.

Starowicz, M., Koutsidis, G., Zielinski, H., 2018. Sensory analysis and aroma compounds of buckwheat containing products-a review. Crit. Rev. Food Sci. Nutr. 58 (11), 1767–1779. https://doi.org/10.1080/10408398.2017.1284742.

Tang, Z., Fan, J., Zhang, Z., Zhang, W., Yang, J., Liu, L., et al., 2021. Insights into the structural characteristics and in vitro starch digestibility on steamed rice bread as affected by the addition of okara. Food Hydrocolloids 113. https://doi.org/10.1016/j.foodhyd.2020.106533.

Tao, H., Fang, X.H., Chen, P., Yang, B.Q., Feng, R., Zhang, B., 2024. Casein/butyrylated dextrin nanoparticles and chitosan stabilized bilayer emulsions as fat substitutes in sponge cakes. Food Chem. 448, 139043 https://doi.org/10.1016/j.foodchem.2024.139043.

Wang, B., Dong, Y., Fang, Y., Gao, W., Kang, X., Liu, P., et al., 2022. Effects of different moisture contents on the structure and properties of corn starch during extrusion. Food Chem. 368, 130804 https://doi.org/10.1016/j.foodchem.2021.130804.

Wang, C., Zhu, Z., Mei, L., Xia, Y., Chen, X., Mustafa, S., Du, X., 2023. The structural properties and resistant digestibility of maize starch-glyceride monostearate complexes. Int. J. Biol. Macromol. 249, 126141 https://doi.org/10.1016/j.ijbiomac.2023.126141.

Wang, J., Ren, F., Yu, J., Copeland, L., Wang, S., 2021. Octenyl succinate modification of starch enhances the Formation of starch-lipid complexes. J. Agric. Food Chem. 69 (49), 14938–14950. https://doi.org/10.1021/acs.jafc.1c05816.

Wang, S., Wang, J., Zhang, W., Li, C., Yu, J., Wang, S., 2015. Molecular order and functional properties of starches from three waxy wheat varieties grown in China. Food Chem. 181, 43–50. https://doi.org/10.1016/j.foodchem.2015.02.065.

Wang, X., Hao, Z., Liu, N., Jin, Y., Wang, B., Bian, Y., et al., 2024. Influence of the structure and physicochemical properties of OSA modified highland barley starch based on ball milling assisted treatment. Int. J. Biol. Macromol. 259 (Pt 1), 129243 https://doi.org/10.1016/j.ijbiomac.2024.129243.

Wei, Q., Zheng, H., Han, X., Zheng, C., Huang, C., Jin, Z., et al., 2023. Octenyl succinic anhydride modified starch with excellent emulsifying properties prepared by selective hydrolysis of supramolecular immobilized enzyme. Int. J. Biol. Macromol. 232, 123383 https://doi.org/10.1016/j.ijbiomac.2023.123383.

Xu, H., Hao, Z., Gao, J., Zhou, Q., Li, W., Liao, X., et al., 2023. Complexation between rice starch and cellulose nanocrystal from black tea residues: gelatinization properties and digestibility in vitro. Int. J. Biol. Macromol. 234, 123695 https://doi.org/10.1016/j.ijbiomac.2023.123695.

Yan, Y., Chen, S., Deng, L., Duan, Y., Huang, Z., Gong, D., Zhang, G., 2024. Construction and characterization of egg white protein-gallic acid-xanthan gum-based emulsion and oleogel. Food Hydrocolloids 150. https://doi.org/10.1016/j.foodhyd.2023.109720.

Yan, Y., Feng, L., Shi, M., Cui, C., Liu, Y., 2020. Effect of plasma-activated water on the structure and in vitro digestibility of waxy and normal maize starches during heat-moisture treatment. Food Chem. 306, 125589 https://doi.org/10.1016/j.foodchem.2019.125589.

Zhang, G., Xuan, Y., Lyu, F., Ding, Y., 2023. Microstructural, physicochemical properties and starch digestibility of brown rice flour treated with extrusion and heat moisture. Int. J. Biol. Macromol. 242 (Pt 1), 124594 https://doi.org/10.1016/j.ijbiomac.2023.124594.

Zhang, R., Zhang, Y., Yu, J., Gao, Y., Mao, L., 2022. Rheology and tribology of ethylcellulose-based oleogels and W/O emulsions as fat substitutes: role of glycerol monostearate. Foods 11 (15). https://doi.org/10.3390/foods11152364.

Zhao, W., Wei, Z., Xue, C., Meng, Y., 2023. Development of food-grade oleogel via the aerogel-templated method: oxidation stability, astaxanthin delivery and emulsifying application. Food Hydrocolloids 134. https://doi.org/10.1016/j.foodhyd.2022.108058.

Zheng, L., Zhong, J., Liu, X., Wang, Q., Qin, X., 2023. Physicochemical properties and intermolecular interactions of a novel diacylglycerol oil oleogel made with ethyl cellulose as affected by γ-oryzanol. Food Hydrocolloids 138. https://doi.org/10.1016/j.foodhyd.2023.108484.

Zheng, X.Q., Wang, D.D., Xue, S., Cui, Z.Y., Yu, H.Y., Wei, J.T., et al., 2024. Composite formation of whey protein isolate and OSA starch for fabricating high internal phase emulsion: a comparative study at different pH and their application in biscuits. Int. J. Biol. Macromol. 259 (Pt 1), 129094 https://doi.org/10.1016/j.ijbiomac.2023.129094.

Zhi-hao, Z., Ai-min, S., Rui, G., Hong-zhi, L., Hui, H., Qiang, W., 2022. Protective effect of high-oleic acid peanut oil and extra-virgin olive oil in rats with diet-induced metabolic syndrome by regulating branched-chain amino acids metabolism. J. Integr. Agric. 21 (3), 878–891.